line-90 by serine) predominates in subjects with platelet GPIV deficiency. Thromb Haemost 69 : 481-484, 1993
19) Nakao S, Takenaka T, Maeda M, et al : An atypical variant of Fabry's disease in men with left ventricular hypertrophy. N Engl J Med 333 : 288-293, 1995
20) Hirano K, Ikeda Y, Zaima N, et al : Triglyceride deposit cardiomyovasculopagthy. N Engl J Med 359 : 2396-2388, 2008
21) Hirano K : A novel clinical entity : Triglyceride deposit cardiomyovasculopagthy 16 : 705-709, 2009
22) Oshima Y, Hirota H, Nagai H, et al : Images in cardiovascular medicine. Specific cardiomyopathy caused by multisystemic lipid storage in Jordan's anomaly. Circulation 106 : 280-281, 2002

THE JOURNAL OF BIOLOGICAL CHEMISTRY VOL. 286, NO. 37, pp. 32045–32053, September 16, 2011

Reduced Expression of Adipose Triglyceride Lipase Enhances Tumor Necrosis Factor α-induced Intercellular Adhesion Molecule-1 Expression in Human Aortic Endothelial Cells via Protein Kinase C-dependent Activation of Nuclear Factor-κB*

Received for publication, July 25, 2011, and in revised form, July 31, 2011 Published, JBC Papers in Press, August 2, 2011, DOI 10.1074/jbc.M111.285650

Tomoaki Inoue[‡], Kunihisa Kobayashi[‡§1], Toyoshi Inoguchi[‡¶], Noriyuki Sonoda[‡¶], Masakazu Fujii[‡], Yasutaka Maeda[‡], Yoshinori Fujimura[¶], Daisuke Miura[¶], Ken-ichi Hirano[‖], and Ryoichi Takayanagi[‡]

From the [‡]Department of Medicine and Bioregulatory Science, Graduate School of Medical Sciences, Kyushu University, 3-1-1 Maidashi, Higashi-ku, Fukuoka 812-8582, Japan, the [§]Department of Endocrinology and Diabetes Mellitus, Fukuoka University Chikushi Hospital, 1-1-1 Zokumyoin, Chikushino, Fukuoka 818-8502, Japan, the [¶]Innovation Center for Medical Redox Navigation, Kyushu University, 3-1-1 Maidashi, Higashi-ku, Fukuoka 812-8582, Japan, and the [‖]Department of Cardiovascular Medicine, Graduate School of Medicine, Osaka University, 2-2 Yamadaoka, Suita, Osaka 565-0871, Japan

Background: Adipose triglyceride lipase (ATGL) expression is decreased in the obese insulin-resistant state.
Results: RNA interference-mediated down-regulation of ATGL enhanced monocyte adhesion via increased expression of tumor necrosis factor α-induced intercellular adhesion molecule-1.
Conclusion: Reduced ATGL expression may influence the atherogenic process in the insulin-resistant state.
Significance: This mechanism also leads to the acceleration of atherosclerosis in patients with insulin-resistance, even if not in a state of hyperglycemia.

We examined the effects of adipose triglyceride lipase (ATGL) on the initiation of atherosclerosis. ATGL was recently identified as a rate-limiting triglyceride (TG) lipase. Mutations in the human ATGL gene are associated with neutral lipid storage disease with myopathy, a rare genetic disease characterized by excessive accumulation of TG in multiple tissues. The cardiac phenotype, known as triglyceride deposit cardiomyovasculopathy, shows massive TG accumulation in both coronary atherosclerotic lesions and the myocardium. Recent reports show that myocardial triglyceride content is significantly higher in patients with prediabetes or diabetes and that ATGL expression is decreased in the obese insulin-resistant state. Therefore, we investigated the effect of decreased ATGL activity on the development of atherosclerosis using human aortic endothelial cells. We found that ATGL knockdown enhanced monocyte adhesion via increased expression of TNFα-induced intercellular adhesion molecule-1 (ICAM-1). Next, we determined the pathways (MAPK, PKC, or NFκB) involved in ICAM-1 up-regulation induced by ATGL knockdown. Both phosphorylation of PKC and degradation of IκBα were increased in ATGL knockdown human aortic endothelial cells. In addition, intracellular diacylglycerol levels and free fatty acid uptake via CD36 were significantly increased in these cells. Inhibition of the PKC pathway using calphostin C and GF109203X suppressed TNFα-induced ICAM-1 expression. In conclusion, we showed that ATGL knockdown increased monocyte adhesion to the endothelium through enhanced TNFα-induced ICAM-1 expression via activation of NFκB and PKC. These results suggest that reduced ATGL expression may influence the atherogenic process in neutral lipid storage diseases and in the insulin-resistant state.

Heart diseases, including coronary heart disease, cardiomyopathy, and heart failure, are the major causes of early mortality in individuals with diabetes mellitus. Despite recent progress in medical, interventional, and surgical treatments, the prognoses for these heart diseases are still worse in diabetics than in non-diabetics; thus, it is important to further elucidate the pathophysiology and mechanisms underlying diabetes-related heart diseases and to identify a novel therapeutic target.

Myocardial triglyceride (TG)[2] content is significantly higher in patients with prediabetes or diabetes than in healthy volunteers (1, 2) and is associated with impaired left ventricular diastolic function (1). However, the role played by TG accumulation in atherosclerosis, including that of the coronary arteries, remains unknown.

Neutral lipid storage disease with myopathy is characterized by the presence of intracellular TG deposition in most tissues due to mutations in adipose triglyceride lipase (ATGL) (3), which catalyzes the first step in the hydrolysis of TG stored within lipid droplets (4). Triglyceride deposit cardiomyovasculopathy, a cardiac phenotype of neutral lipid storage disease with myopathy, shows TG accumulation in the coronary arteries and the myocardium, leading to concentric and diffuse coronary atherosclerotic lesions and chronic heart failure, both common in diabetics. Because the expression and enzymatic

* This work was supported by research grants-in-aid for rare and intractable diseases from the Ministry of Health, Labor, and Welfare of the Japanese Government (to K. H. and K. K.).
[1] To whom correspondence should be addressed: 1-1-1 Zokumyoin, Chikushino, Fukuoka 818-8502, Japan. Tel.: 81-92-921-1011; Fax: 81-92-928-0856; E-mail: nihisak@fukuoka-u.ac.jp.

[2] The abbreviations used are: TG, triglyceride; ATGL, adipose triglyceride lipase; ICAM, intercellular adhesion molecule; NFκB, nuclear factor-κB; HSL, hormone-sensitive lipase; DAG, diacylglycerol; VCAM, vascular cell adhesion molecule.

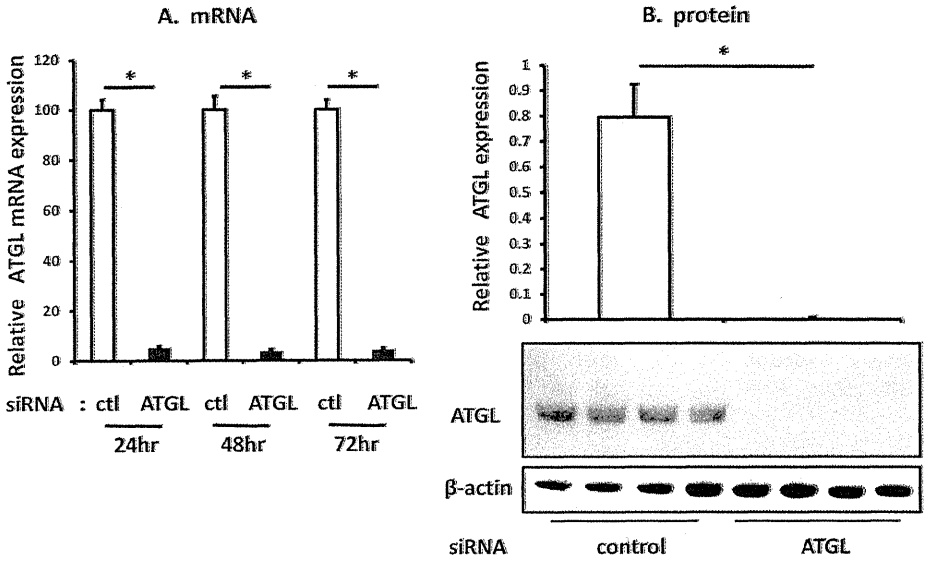

FIGURE 1. **RNAi-induced ablation of ATGL in HAECs.** HAECs were transfected with double-stranded ATGL-specific siRNA at a final concentration of 50 nM and cultured for 24–72 h at 37 °C. Control HAECs were incubated with the siRNA-negative universal control. *A*, ATGL and β-actin mRNA were evaluated using real-time RT-PCR. *Bars*, mean ± S.E. (*error bars*) ($n = 10$); *, $p < 0.0001$ *versus* control. *B*, Western blots (after SDS-PAGE separation of 30 μg of HAEC cell protein) were developed using anti-ATGL or anti-β-actin antibodies. *Bars*, mean ± S.E. (*error bars*) ($n = 5$). *, $p < 0.001$ *versus* control. *Open bars*, control siRNA; *closed bars*, ATGL siRNA.

activity of the ATGL protein are reduced in obese subjects and in the insulin-resistant state (5, 6), ATGL may be related to the high incidence of accelerated atherosclerosis and cardiomyopathy seen in individuals with diabetes mellitus.

Several adhesion molecules are expressed on endothelial cells and play an important role in monocyte-endothelium interactions during the initiation and progression of atherosclerosis. intercellular adhesion molecule-1 (ICAM-1), a member of the immunoglobulin supergene family, is involved in immune and inflammatory responses (7) because it is critical for mediating monocyte adhesion to the endothelium (8) and the transmigration of leukocytes. A previous study (9) reported elevated levels of ICAM-1 in diabetes. Also, nuclear transcription factor-κB (NFκB) is an important factor involved in the transcriptional regulation of ICAM-1 stimulated by tumor necrosis factor α (TNFα) (10). In this report, we investigated how ATGL knockdown affected monocyte adhesion to the endothelium and TNFα-induced ICAM-1 expression and NFκB activation in human aortic endothelial cells (HAECs).

EXPERIMENTAL PROCEDURES

Materials—Anti-ATGL, anti-IκBα, anti-NFκB p65, phosphospecific anti-Akt, phosphospecific anti-JNK, anti-JNK, phosphospecific anti-p38, anti-p38, and phosphospecific anti-pan-protein kinase C (PKC) (α, βI, βII, γ, δ, ϵ, η, θ, ζ, and ι) antibodies were purchased from Cell Signaling (Danvers, MA). Anti-ICAM-1, anti-CD36, and phosphospecific anti-hormone-sensitive lipase (HSL) antibodies were obtained from Abcam (Cambridge, UK). The anti-pan-PKC antibody was purchased from Novus Biologicals (Littleton, CO). Anti-Akt, anti-β-actin, and horseradish peroxidase-conjugated anti-goat secondary antibodies were obtained from Santa Cruz Biotechnology, Inc. (Santa Cruz, CA). Horseradish peroxidase-conjugated anti-mouse and -rabbit secondary antibodies were obtained from Amersham Biosciences. The PKC inhibitors, calphostin C and GF109203X, were purchased from Biomol Research Laboratories (Plymouth Meeting, PA). All other reagents were purchased from Sigma.

Cells—HAECs were obtained from Cambrex (Walkersville, MD) and grown in 75-cm^2 culture flasks (250,000 cells/flask) (Corning Glass) at 37 °C in 5% CO_2 in endothelial basal medium-2 supplemented with endothelial cell growth medium SingleQuots (Cambrex). HAECs were used at passages five or six. Human monocytic U937 cells were purchased from the Human Sciences Research Resource Bank (Tokyo, Japan) and grown in RPMI 1640 medium (Sigma) containing 10% fetal bovine serum (Hyclone, Victoria, Australia), 100 units/ml penicillin, 100 μg/ml streptomycin, and 2 mM L-glutamine at 37 °C in a humidified atmosphere of 95% air and 5% CO_2.

Small Interfering RNA Transfection—HAECs were plated at a density that achieved 50–80% confluence on the day of transfection. Lipofectamine RNAiMAX (Invitrogen) and ATGL Stealth siRNA or a Stealth siRNA-negative universal control (Invitrogen) were first incubated in Opti-MEM I reduced serum medium (Invitrogen) and added to the HAECs in antibiotic-free medium. Nucleotides 575–599 (GenBank™ accession number NM020376) of human ATGL cDNA (5′-GAGAATGTCATTATATCCCACTTCA-3′) were used as the target sequence for RNAi-mediated knockdown.

Monocyte Adhesion Assay—HAECs were grown in 6-well plates and transfected with control siRNA or ATGL siRNA. On the day of the experiment, the medium was removed from each well, the cells were washed with PBS, and fresh medium containing U937 cells (3×10^5 cells/well) was added to each well and incubated for 15 min at room temperature on a rocking plate. After washing with PBS, adherent U937 cells were fixed in 1% paraformaldehyde. The number of adherent cells was

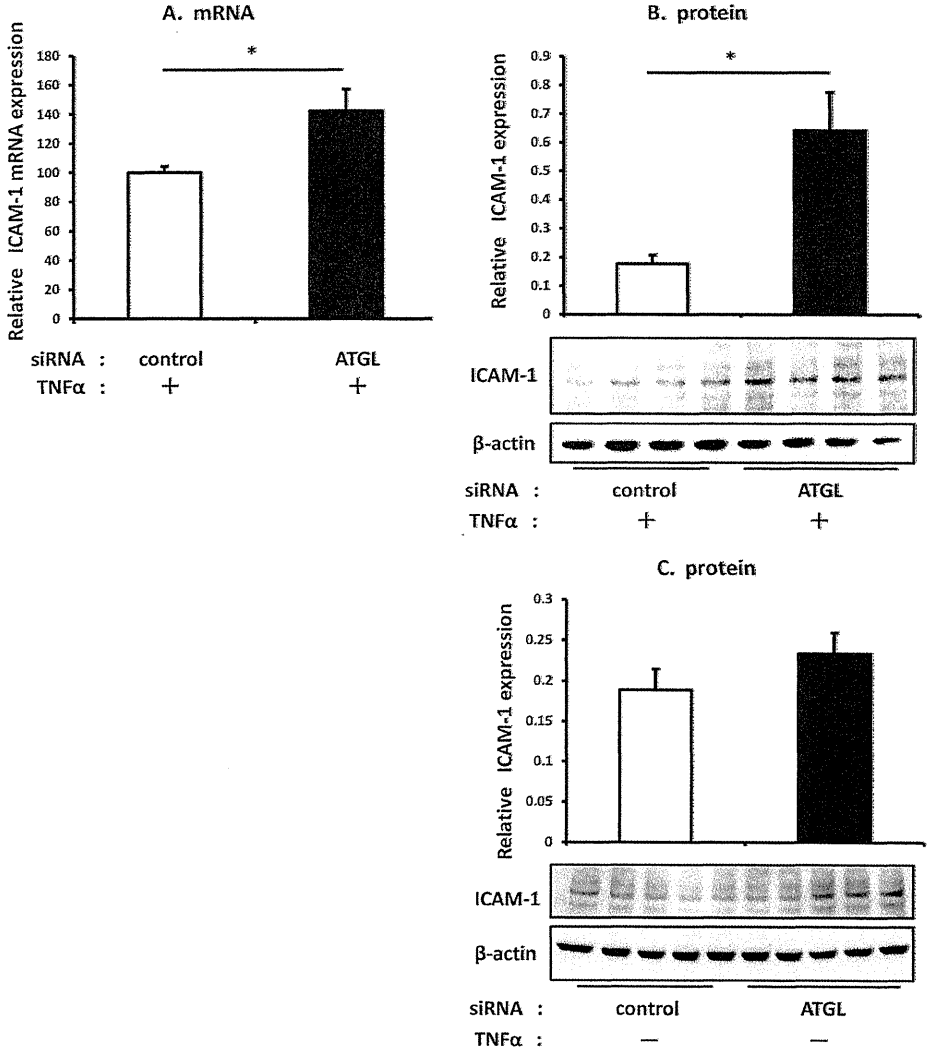

FIGURE 2. **Knockdown of ATGL increased TNFα-induced ICAM-1 expression in HAECs.** HAECs were transfected with either control or ATGL siRNA for 6 h and then treated with or without 1 ng/ml TNFα for 18 h. *A*, the levels of ICAM-1 and β-actin mRNA were evaluated using real-time RT-PCR. *Bars*, mean ± S.E. (*error bars*) ($n = 10$); *, $p < 0.05$ *versus* control. *B* and *C*, Western blots (after SDS-PAGE separation of 30 μg of HAEC cell protein) were developed using anti-ICAM-1 or anti-β-actin antibodies. *Bars*, mean ± S.E. (*error bars*) ($n = 5$). *, $p < 0.05$ *versus* control. *Open bars*, control siRNA; *closed bars*, ATGL siRNA.

counted in five different fields using an ocular grid (0.01 mm^2/field).

RNA Extraction and Quantitative RT-PCR—HAECs were plated at 1.7×10^4/well in 24-well plates in endothelial basal medium-2 for 24 h at 37 °C (50–60% confluent). HAECs were then transfected with control siRNA or ATGL siRNA and stimulated with TNFα. Total RNA was purified using an RNeasy Plus minikit (Qiagen, Valencia, CA) according to the manufacturer's instructions. Extracted RNA (4 μg) was converted to single-stranded cDNA using a QuantiTect reverse transcription kit (Qiagen). The mRNA levels were quantified by quantitative RT-PCR using iTaq SYBR Green mix (Bio-Rad) and the Bio-Rad Chromo 4/Opticon system. The following primer pairs were used: ATGL, 5′-GTGTCAGACGGCGAGAATG-3′ (sense) and 5′-TGGAGGGAGGGAGGGATG-3′ (antisense); ICAM-1, 5′-CAGAAGAAGTGGCCCTCCATAG-3′ (sense) and 5′-GGGCCTTTGTGTTTTGATGCTA-3′ (antisense); CD36, 5′-GGGCTATAGGGATCCATTTTTG-3′ (sense) and 5′-CCTTTCAGATTAACGTCGGATTC-3′ (antisense); peroxisome proliferator-activated receptor γ (PPARγ), 5′-GCTGTGCAGGAGATCACAGA-3′ (sense) and 5′-GGGCTCCATAAAGTCACCAA-3′ (antisense); HSL, 5′-ACTGCCAGCTGCCTTAAAAA-3′ (sense) and 5′-CCTCTGGTGTGGTTCAGGTT-3′ (antisense); β-actin, 5′-GGACTTCGAGCAAGAGATGG-3′ (sense) and 5′-AGCACTGTGTTGGCGTACAG-3′ (antisense).

The linearity of the amplifications as a function of cycle number was tested in preliminary experiments, and the mRNA expression levels were normalized to the expression levels of the housekeeping gene β-actin.

Western Blot Analysis—Cells were lysed in lysis buffer (50 mM Tris-HCl, pH 7.4, 150 mM NaCl, 5 mM sodium fluoride, 0.25 mM EDTA, pH 8.0, 1% deoxycholic acid, 1% Triton X-100, 1 mM sodium orthovanadate) supplemented with a protease inhibitor mixture (Sigma) and phosphatase inhibitors (Sigma). Samples were then separated on 10% SDS-polyacrylamide gels (Bio-Rad) and transferred onto 0.2-μm polyvinyl difluoride membranes (Bio-Rad) in Tris/glycine buffer. The membranes were exposed

to primary antibodies followed by secondary antibodies conjugated to HRP. Signals were detected using a chemiluminescent reaction (ECL Plus, Amersham Biosciences). The primary antibodies used were anti-ATGL rabbit polyclonal antibody (1:1000), anti-ICAM-1 mouse monoclonal antibody (1:3000), anti-IκBα rabbit polyclonal antibody (1:1000), anti-p65 NFκB rabbit monoclonal antibody (1:2000), phosphospecific anti-Akt mouse monoclonal antibody (1:1000), anti-Akt goat polyclonal antibody (1:200), phosphospecific anti-JNK mouse monoclonal antibody (1:2000), anti-JNK rabbit monoclonal antibody (1:1000), phosphospecific anti-p38 MAPK rabbit monoclonal antibody (1:1000), anti-p38 MAPK rabbit polyclonal antibody (1:1000), phosphospecific anti-pan-PKC rabbit monoclonal antibody (1:1000), anti-pan-PKC rabbit polyclonal antibody, anti-CD36 rabbit polyclonal antibody (1:1000), phosphospecific anti-HSL rabbit polyclonal antibody (1:1000), and anti-β-actin mouse polyclonal antibody (1:10,000). In several of the experiments, the cells were incubated for 30 min with the PKC inhibitors, calphostin C and GF109203X, before TNFα stimulation.

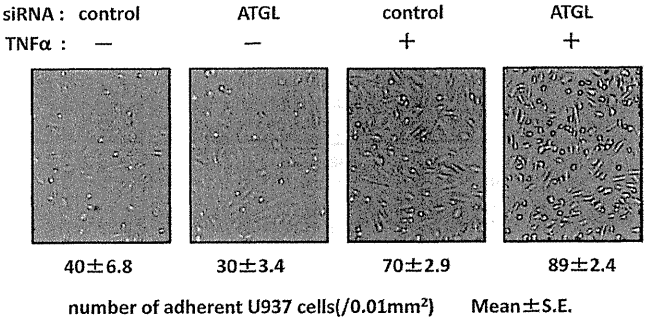

FIGURE 3. **Effects of ATGL knockdown on U937 cell adhesion to TNFα-stimulated HAECs.** HAECs were transfected with control or ATGL siRNA for 6 h and then incubated with or without TNFα (1 ng/ml) for 18 h. U937 cells were incubated on each monolayer for 15 min. The number of adherent U937 cells within a high power field (0.01 mm²/field) was counted. Photographs represent randomly chosen fields from three separate experiments. Data represent the mean ± S.E. of five different fields.

Measurement of Intracellular Diglycerides—Cells were harvested and washed twice with 150 mM NaCl, and total lipids were extracted using the Folch partition method (11). Briefly, cells were dissolved in 7.5 ml of chloroform/methanol/water (8:4:3, v/v/v) and allowed to stand for 30 min at room temperature. After centrifugation at 500 × *g* for 10 min, the lower phase was collected. The upper phase was mixed with 4 ml of chloroform, and diacylglycerol (DAG) was re-extracted as outlined above. The lower phases (containing lipid) from the two centrifugation steps were combined and dried under nitrogen gas. Total diacylglycerol content and that of the various molecular species of diacylglycerol were measured using high performance liquid chromatography-tandem mass spectrometry, as described previously (12).

Labeling of DAG—HAECs were incubated with medium containing 2% fetal bovine serum (FBS) and [^{3}H]palmitate (20 μCi/ml). The reaction was terminated, and total lipids were extracted as described above. First, the radioactivity of the total cell lipid extract was measured to evaluate the effects of ATGL knockdown on the incorporation of labeled fatty acids into the cells. Next, labeled DAG was separated on silica gel G thin layer plates developed in hexane/ether/acetic acid (60:40:1). The DAG spots (visualized using iodine gas) were scraped, and the radioactivity of the samples was determined by liquid scintillation counting (13).

Statistical Analysis—All data were expressed as the mean ± S.E. Statistical analysis was performed using Student's *t* test, and $p < 0.05$ was considered statistically significant.

RESULTS

ATGL Knockdown Increases TNFα-induced ICAM-1 Expression—Adhesion of circulating monocytes to the endothelium is one of the key events during the early stages of atherosclerogenesis (14). Because ICAM-1 mediates monocyte adhesion to the endothelium, we examined the expression of TNFα-induced ICAM-1 in ATGL knockdown HAECs. As shown in Fig. 1*A*, 24–72 h after siRNA transfection, we observed a >95% decrease in ATGL mRNA expression in

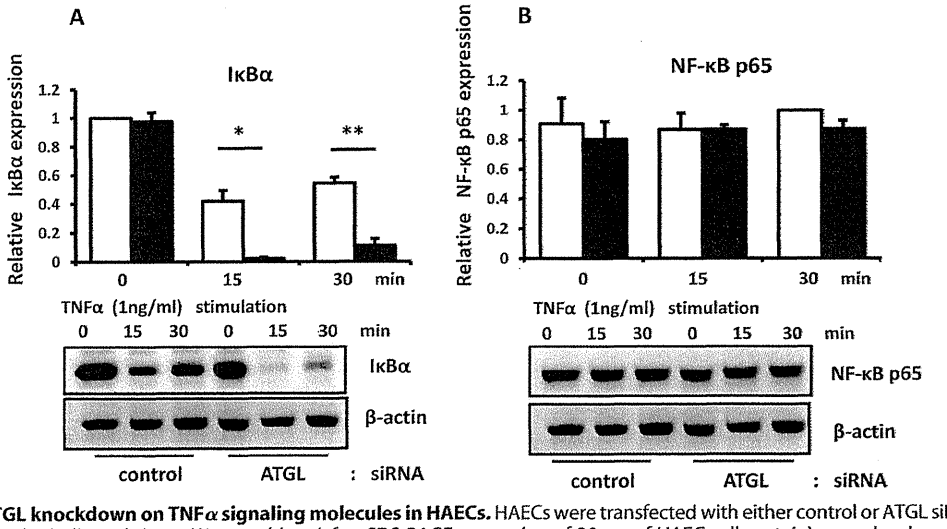

FIGURE 4. **Effects of ATGL knockdown on TNFα signaling molecules in HAECs.** HAECs were transfected with either control or ATGL siRNA and then treated with TNFα (1 ng/ml) for the indicated times. Western blots (after SDS-PAGE separation of 30 μg of HAEC cell protein) were developed using anti-IκBα (*A*), anti-NFκB p65 (*B*), or anti-β-actin antibodies. *Bars*, mean ± S.E. (*error bars*) ($n = 3$). The *bar graphs* represent the percentage of the maximum from three independent experiments. *, $p < 0.05$; **, $p < 0.005$ *versus* control. *Open bars*, control siRNA; *closed bars*, ATGL siRNA.

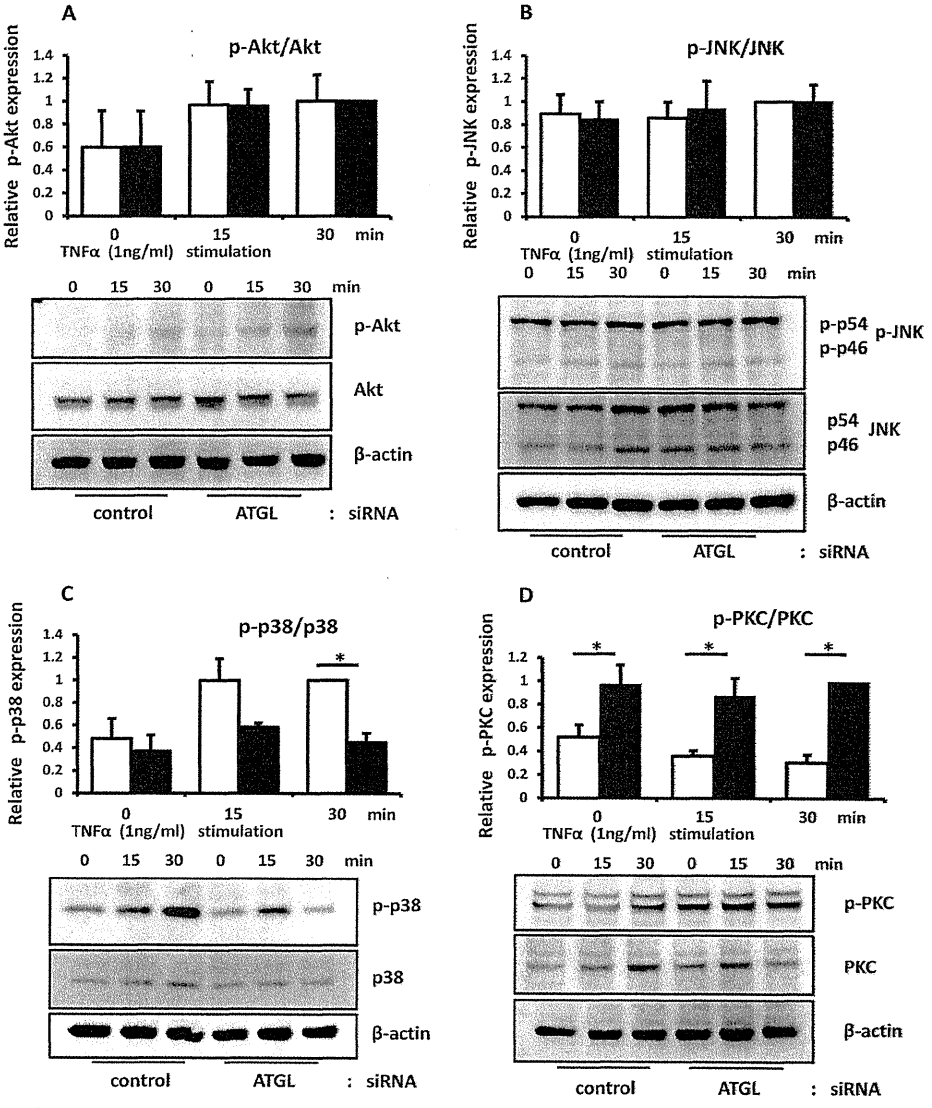

FIGURE 5. **Phosphorylated forms of Akt, JNK kinase, p38 kinase, or PKC induced by TNFα (1 ng/ml) in ATGL knockdown HAECs.** HAECs were transfected with either control or ATGL siRNA and then treated with TNFα (1 ng/ml) for the indicated times. Western blots (after SDS-PAGE separation of 20 μg of HAEC cell protein) were developed using anti-phospho-Akt (*A*), anti-phospho-JNK (*B*), anti-phospho-p38 (*C*), anti-phospho-PKC (*D*), or anti-β-actin antibodies. *Bars*, mean ± S.E. (*error bars*) ($n = 4$). The *bar graphs* represent the percentage of the maximum from four independent experiments. *, $p < 0.05$ *versus* control. *Open bars*, control siRNA; *closed bars*, ATGL siRNA.

ATGL knockdown cells compared with that in cells transfected with the control. ATGL protein expression also decreased in ATGL knockdown HAECs 24 h after transfection (Fig. 1*B*). We next found that both the mRNA and protein levels of TNFα-induced ICAM-1 increased in HAECs treated with ATGL siRNA (Fig. 2, *A* and *B*). ATGL knockdown alone had no significant effect on ICAM-1 levels (Fig. 2*C*). Next, we examined whether ATGL knockdown affected TNFα-stimulated adhesion of human monocytoid U937 cells to HAECs. As shown in Fig. 3, treatment of HAECs with TNFα (1 ng/ml) for 18 h resulted in a marked increase in the adhesion of U937 cells. ATGL knockdown alone had no significant effect on U937 cell adhesion, but it significantly increased the number of U937 cells adhering to HAECs in the presence of TNFα.

The Signal Transduction Pathway Leading to Synthesis of Adhesion Molecules Involves Activation of NFκB—NFκB activation by inflammatory cytokines (including TNFα) results in the induction of various endothelial cell adhesion molecules, such as vascular cell adhesion molecule-1 (VCAM-1), E-selectin, and ICAM-1. These molecules participate in the recruitment of leukocytes to inflammatory lesions (10, 15). We next determined the effect of ATGL knockdown on the degradation of IκBα and the expression of NFκB in HAECs and found that the amount of IκBα protein was markedly decreased 15 min after TNFα stimulation (Fig. 4*A*). Pretreatment with ATGL siRNA significantly increased TNFα-mediated degradation of IκBα at 15 and 30 min but did not affect the expression of NFκB (Fig. 4*B*).

Effect of ATGL Knockdown on Akt-, MAPK-, and PKC-enhanced NFκB Signaling in HAECs—To determine which kinase is involved in IκBα degradation, we examined several kinases, including JNK, p38 MAPK, Akt, and PKC (16–18). ATGL knockdown had no effect on the phosphorylation of Akt and JNK1/2, whereas phosphorylation of p38 was decreased (Fig. 5, *A–C*). In contrast, phosphorylation of PKC was increased in

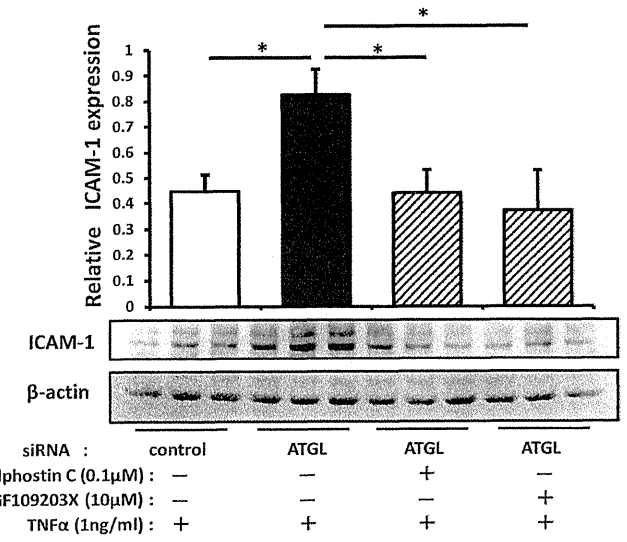

FIGURE 6. **Inhibition of PKC prevented TNFα-induced ICAM-1 up-regulation in ATGL knockdown HAECs.** HAECs were transfected with either control or ATGL siRNA for 6 h and then treated with or without the indicated inhibitors (0.10 μM calphostin C, 10 μM GF109203X) for 30 min followed by incubation with 1 ng/ml TNFα for 17.5 h. Western blots (after SDS-PAGE separation of 30 μg of HAEC cell protein) were developed using anti-ICAM-1 or anti-β-actin antibodies. *Bars*, mean ± S.E. ($n = 6$). *, $p < 0.05$ *versus* control. *Open bars*, control siRNA; *closed bars*, ATGL siRNA; *hatched bars*, PKC inhibitors.

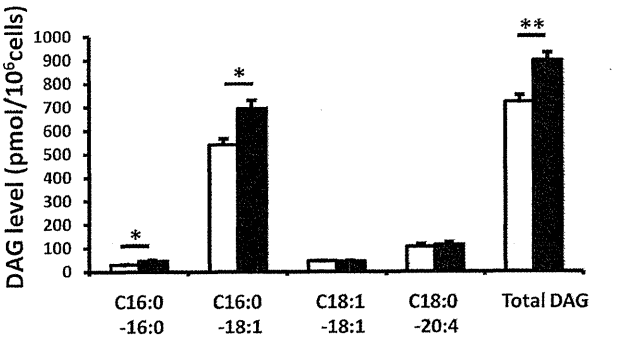

FIGURE 7. **Knockdown of ATGL increased the diglyceride content of HAECs.** HAECs were transfected with either control or ATGL siRNA. Total DAG levels and those of the individual classes of DAG were determined using high performance liquid chromatography-tandem mass spectrometry. *Bars*, mean ± S.E. (*error bars*) ($n = 5$). *, $p < 0.01$; **, $p < 0.005$ *versus* control. *Open bars*, control siRNA; *closed bars*, ATGL siRNA.

ATGL knockdown HAECs (Fig. 5*D*). Pretreatment of HAECs with calphostin C (0.1 μM) and GF109203X (10 μM) completely abrogated TNFα-induced ICAM-1 up-regulation in ATGL knockdown HAECs (Fig. 6). These data suggest that TNFα-induced ICAM-1 up-regulation is PKC-dependent.

Effect of ATGL Knockdown on Diacylglycerol Metabolism—Free fatty acids activate PKC via increased synthesis of DAG, a potent activator of PKC (19, 20). We next examined the effect of ATGL knockdown on DAG levels and found that total DAG levels were increased 1.3-fold in ATGL knockdown HAECs (Fig. 7). We also observed significantly higher levels of 1-palmitoyl-2-oleoylglycerol (C16:0–18:1) and 1,2-dioleoylglycerol (C16:0–16:0)(Fig. 7). Next, labeling studies were used to further examine the mechanisms underlying the increase in DAG. ATGL knockdown increased the incorporation of [^{3}H]palmitate into HAECs (Fig. 8*A*). Furthermore, the level of labeled DAG in ATGL knockdown HAECs significantly increased when the cells were incubated with [^{3}H]palmitate (Fig. 8*B*). Because transmembrane transport of free fatty acids is actively facilitated by transporter proteins, we examined the gene expression of the fatty acid transporter, CD36. CD36 expression increased dramatically in ATGL knockdown HAECs (Fig. 9, *A* and *B*). PPARγ is essential for the basal regulation of CD36, and many factors regulate CD36 expression through a PPARγ-dependent mechanism (21). We found that ATGL knockdown increased PPARγ mRNA expression in HAECs (Fig. 10). Taken together, these data demonstrate that DAG synthesis increases via increased CD36-mediated fatty acid transportation in ATGL knockdown HAECs.

The classical enzyme, HSL, hydrolyzes TG, DAG, and monoacylglyceride but has highest specific activity against DAG (22). We next determined the effect of ATGL knockdown on HSL activation. The expression levels of HSL mRNA and HSL phosphoprotein were unchanged in ATGL knockdown HAECs (Fig. 11, *A* and *B*). This suggests that increased DAG synthesis, along with an impaired compensatory increase in HSL-mediated DAG hydrolysis, may contribute to increased DAG levels in ATGL knockdown HAECs.

DISCUSSION

Heart diseases, including ischemic heart disease and heart failure, are the major cause of mortality in diabetics, despite recent developments in medical and surgical treatment. Therefore, it is important to elucidate the underlying mechanisms and to identify new therapeutic targets. Increased TG levels in plasma and tissues are a common feature of the diabetic state. This abnormal TG metabolism may contribute to heart diseases in diabetics. Lingvay *et al.* (23) reported that increased TG content in the myocardium, a common feature in diabetics, is associated with ventricular diastolic dysfunction. However, it remains unclear whether TG deposition plays a role in the process of atherosclerosis. To clarify this, we focused our attention on ATGL, a recently discovered TG lipase (4). ATGL is the causative gene of triglyceride deposit cardiomyovasculopathy, which is characterized by massive accumulation of TG in the coronary arteries and myocardium and leads to chronic heart failure (24). Additionally, in patients with prediabetes or diabetes, ATGL protein expression and TG lipase activity are both reduced (5, 6). Therefore, we investigated whether decreased ATGL activity may affect several biomolecules involved in the process of atherosclerosis *in vitro*.

Endothelial cell activation by various inflammatory stimuli, including TNFα, increases the adherence of monocytes, a crucial step in the development of vascular diseases (15). We assessed the effect of ATGL activity on U937 adhesion to HAECs stimulated with TNFα. Our results show that ATGL knockdown in HAECs stimulated with TNFα up-regulates the expression of the adhesion molecule, ICAM-1, resulting in enhanced monocyte adhesion. This finding indicates that ATGL acts as an endogenous modulator of endothelial inflammatory responses and the adherence of monocytes.

NFκB regulates the expression of numerous proteins involved in inflammation, including cytokines (IL-6), chemokines (IL-8, MCP-1, and regulated upon activation, normal T

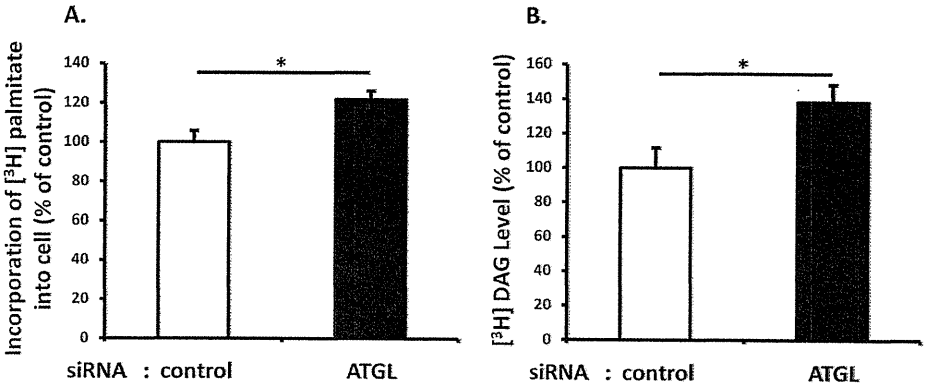

FIGURE 8. **Knockdown of ATGL increased [^{3}H]palmitate incorporation into both cells and intracellular DAG.** HAECs were transfected with either control or ATGL siRNA for 6 h and then incubated for 18 h with medium containing 2% FBS and [^{3}H]palmitate (20 μCi/ml). Total lipids (*A*) were extracted, DAGs (*B*) were separated by thin layer chromatography, and the radioactivity was counted. *Bars*, mean ± S.E. ($n = 5$). *, $p < 0.05$ *versus* control. *Open bars*, control siRNA; *closed bars*, ATGL siRNA.

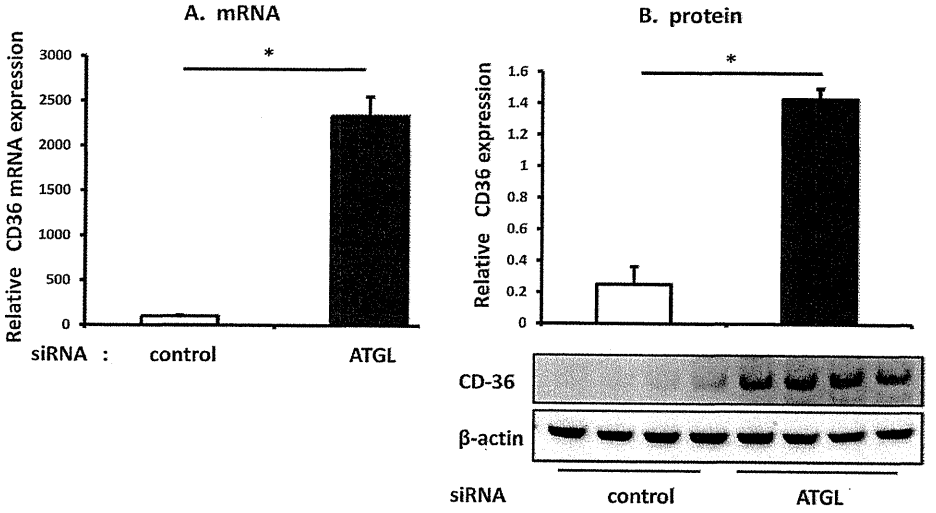

FIGURE 9. **Knockdown of ATGL increased CD36 expression in HAECs.** HAECs were transfected with either control or ATGL siRNA. *A*, CD36 and β-actin mRNA levels were evaluated using real-time RT-PCR. *Bars*, mean ± S.E. ($n = 8$); *, $p < 0.0001$ *versus* control. *B*, Western blots (after SDS-PAGE separation of 30 μg of HAEC cell protein) were developed using anti-CD36 or anti-β-actin antibodies. *Bars*, mean ± S.E. ($n = 5$). *, $p < 0.0001$ *versus* control. *Open bars*, control siRNA; *closed bars*, ATGL siRNA.

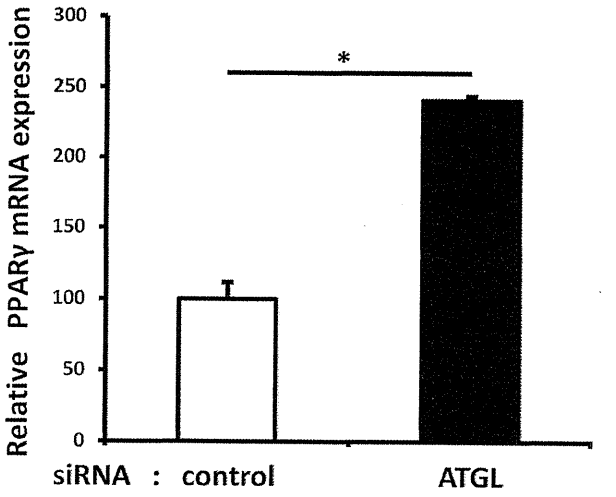

FIGURE 10. **Knockdown of ATGL increased PPARγ mRNA expression in HAECs.** HAECs were transfected with either control or ATGL siRNA. PPARγ and β-actin mRNA levels were evaluated using real-time RT-PCR. *Bars*, mean ± S.E. (*error bars*) ($n = 6$). *, $p < 0.0001$ *versus* control. *Open bars*, control siRNA; *closed bars*, ATGL siRNA.

cell expressed and secreted (RANTES)), and cell adhesion molecules (ICAM-1 and VCAM-1) (25). The NFκB transcription factor is present in the cytosol in an inactive state complexed with the inhibitory protein, IκB (26). Activation occurs via phosphorylation of IκBα at Ser-32 and Ser-36, followed by proteasome-mediated degradation, resulting in the release and nuclear translocation of active NFκB (27). In the present study, we showed that the amount of IκBα protein in ATGL knockdown HAECs was markedly decreased 15 min after TNFα stimulation. These results suggest that ATGL knockdown increases ICAM-1 expression via activation of NFκB. The signaling pathways mediating these effects involve p42/44 MAPK, p38 MAPK, and PKC (28, 29). We showed that phosphorylation of PKC was increased in ATGL knockdown HAECs and that calphostin C and GF109203X inhibit TNFα-induced ICAM-1 expression. We concluded, therefore, that ATGL knockdown-induced expression of ICAM-1 was mediated by PKC-dependent NFκB activation.

PKCs are activated by DAG, phosphatidylserine, and phorbol esters. Although the absence of ATGL would be expected to

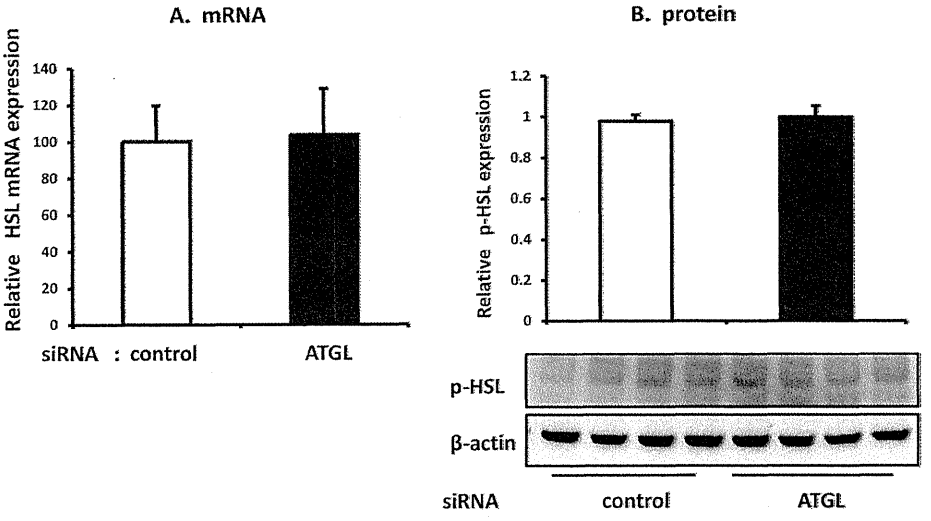

FIGURE 11. **Knockdown of ATGL did not affect HSL mRNA expression and phosphoprotein expression in HAECs.** HAECs were transfected with either control or ATGL siRNA. *A*, HSL and β-actin mRNA levels were evaluated using real-time RT-PCR. *Bars*, mean ± S.E. ($n = 6$). *B*, Western blots (after SDS-PAGE separation of 30 μg of HAEC cell protein) were developed using anti-phospho-HSL or anti-β-actin antibodies. *Bars*, mean ± S.E. ($n = 5$). *Open bars*, control siRNA; *closed bars*, ATGL siRNA.

reduce both TG hydrolysis and other lipid metabolites, DAG concentrations were, surprisingly, increased in ATGL knockout mice (30). We found that PKC was already activated before TNFα stimulation in ATGL knockdown HAECs (Fig. 5*D*). Therefore, we speculated that increased DAG levels induced by ATGL knockdown activate PKC and found that DAG levels were increased in ATGL knockdown HAECs (Fig. 7). Interestingly, the fatty acid composition of DAG derived from *de novo* synthesis is supposed to be rich in palmitate and oleate, whereas DAG derived from phosphatidylinositol breakdown is rich in arachidonate (13, 31). In the present study, we found that the levels of diacylglycerol species containing palmitic acid (C16:0) and oleic acid (C18:1) were increased in ATGL knockdown HAECs, but the levels of diacylglycerol species containing arachidonic acid (C20:4) showed no significant differences (Fig. 7). These findings suggested that DAGs derived from *de novo* synthesis were increased in ATGL knockdown HAECs. We previously reported that saturated non-esterified fatty acids can also stimulate *de novo* DAG synthesis and PKC activity in cultured aortic endothelial cells (32) and vascular smooth muscle cells (19). In the present study, we showed that fatty acid uptake, DAG synthesis, and the expression of CD36 (a major transporter for oxidized low density lipoprotein and long chain fatty acids) were increased in ATGL knockdown HAECs. This suggests that increased DAG synthesis due to uptake of fatty acids via up-regulated CD36 causes PKC activation in ATGL knockdown HAECs. However, we did not determine which isoform of PKC is involved in the regulation. It was reported that enhanced fatty acid flux increases the activation of the PKC isoforms, PKCα/βII, and of NFκB (20). Therefore, PKCα/βII might be involved in PKC activation induced by ATGL knockdown; however, further studies are necessary. Because ATGL hydrolyzes TG, DAG, and monoacylglyceride, the absence of ATGL-mediated DAG hydrolysis, with the absence of a compensatory increase in HSL, may also contribute to increased DAG levels. Additionally, enhanced CD36 expression stimulates the uptake of oxidized low density lipoprotein, leading to the excessive acceleration of atherosclerosis in the presence of low ATGL activity, as seen in insulin resistance and diabetes.

In recent years, oxidative stress has been considered an important pathogenic factor in the development of diabetic vascular complications (33–35). Accumulating evidence shows that many protein, lipid, and DNA markers of oxidative stress are increased in the kidney and vascular tissues from animals and patients with diabetes (35–37). We previously reported that high glucose levels stimulate superoxide production via the PKC-dependent activation of NAD(P)H oxidases in cultured aortic endothelial cells and smooth muscle cells (38). The mechanisms underlying PKC-dependent activation of NAD(P)H oxidase were thought to act via PKC-dependent activation of the small GTPase, Rac-1, which is an important regulator of NAD(P)H oxidase activation (39). Activated PKC phosphorylates $p47^{phox}$ and induces the release of superoxide from NOX components. In the present study, we found that both phosphorylation of PKC and DAG synthesis were increased in ATGL knockdown HAECs, suggesting that reduced ATGL expression may increase oxidative stress mediated by activated PKC without high glucose or increased free fatty acid. This mechanism also leads to the acceleration of atherosclerosis in triglyceride deposit cardiomyovasculopathy and in patients with insulin resistance, even if not in a state of hyperglycemia or increased free fatty acids.

PPARγ is essential for the basal regulation of CD36, and many factors regulate CD36 expression through a PPARγ-dependent mechanism (21). In agreement with another report (21), we found that that PPARγ mRNA expression was increased in ATGL knockdown HAECs.

In conclusion, our results show for the first time that PKC is activated by increased fatty acid uptake and DAG synthesis in ATGL knockdown HAECs, at least in part, via increased expression of CD36. Activation of PKC leads to NFκB activation and, in turn, to increased expression of TNFα-induced ICAM-1 genes. In humans, there are many secretory products from adipocytes, including free fatty acids and TNFα, which are

known to modulate multiple physiological functions. In the obese insulin-resistant state, decreased ATGL activity, coupled with increased TNFα levels, is likely to contribute to the chronic inflammatory events associated with atherosclerosis.

Acknowledgments—We appreciate the technical support provided by the Research Support Center, Graduate School of Medical Sciences, Kyushu University, and the Innovation Center for Medical Redox Navigation, Kyushu University. We also thank Eri Nagashima for secretarial assistance, Mikiko Sato and Arisa Matsuyama for skillful technical assistance, and Dr. Kiyoshi Sakai for technical suggestions.

REFERENCES

1. Rijzewijk, L. J., van der Meer, R. W., Smit, J. W., Diamant, M., Bax, J. J., Hammer, S., Romijn, J. A., de Roos, A., and Lamb, H. J. (2008) *J. Am. Coll. Cardiol.* **52,** 1793–1799
2. McGavock, J. M., Lingvay, I., Zib, I., Tillery, T., Salas, N., Unger, R., Levine, B. D., Raskin, P., Victor, R. G., and Szczepaniak, L. S. (2007) *Circulation* **116,** 1170–1175
3. Kobayashi, K., Inoguchi, T., Maeda, Y., Nakashima, N., Kuwano, A., Eto, E., Ueno, N., Sasaki, S., Sawada, F., Fujii, M., Matoba, Y., Sumiyoshi, S., Kawate, H., and Takayanagi, R. (2008) *J. Clin. Endocrinol. Metab.* **93,** 2877–2884
4. Zimmermann, R., Strauss, J. G., Haemmerle, G., Schoiswohl, G., Birner-Gruenberger, R., Riederer, M., Lass, A., Neuberger, G., Eisenhaber, F., Hermetter, A., and Zechner, R. (2004) *Science* **306,** 1383–1386
5. Jocken, J. W., Langin, D., Smit, E., Saris, W. H., Valle, C., Hul, G. B., Holm, C., Arner, P., and Blaak, E. E. (2007) *J. Clin. Endocrinol. Metab.* **92,** 2292–2299
6. Steinberg, G. R., Kemp, B. E., and Watt, M. J. (2007) *Am. J. Physiol. Endocrinol. Metab.* **293,** E958–E964
7. Casasnovas, J. M., Bickford, J. K., and Springer, T. A. (1998) *J. Virol.* **72,** 6244–6246
8. Kevil, C. G., Patel, R. P., and Bullard, D. C. (2001) *Am. J. Physiol. Cell Physiol.* **281,** C1442–C1447
9. Seckin, D., Ilhan, N., Ilhan, N., and Ertugrul, S. (2006) *Diabetes Res. Clin. Pract.* **73,** 191–197
10. Collins, T., Read, M. A., Neish, A. S., Whitley, M. Z., Thanos, D., and Maniatis, T. (1995) *FASEB J.* **9,** 899–909
11. Folch, J., Lees, M., and Sloane Stanley, G. H. (1957) *J. Biol. Chem.* **226,** 497–509
12. Biclawski, J., Szulc, Z. M., Hannun, Y. A., and Biclawska, A. (2006) *Methods* **39,** 82–91
13. Inoguchi, T., Xia, P., Kunisaki, M., Higashi, S., Feener, E. P., and King, G. L. (1994) *Am. J. Physiol.* **267,** E369–E379
14. Gerrity, R. G. (1981) *Am. J. Pathol.* **103,** 181–190
15. Ross, R. (1993) *Nature* **362,** 801–809
16. Read, M. A., Whitley, M. Z., Gupta, S., Pierce, J. W., Best, J., Davis, R. J., and Collins, T. (1997) *J. Biol. Chem.* **272,** 2753–2761
17. Sluss, H. K., Barrett, T., Dérijard, B., and Davis, R. J. (1994) *Mol. Cell. Biol.* **14,** 8376–8384
18. Ozes, O. N., Mayo, L. D., Gustin, J. A., Pfeffer, S. R., Pfeffer, L. M., and Donner, D. B. (1999) *Nature* **401,** 82–85
19. Yu, H. Y., Inoguchi, T., Kakimoto, M., Nakashima, N., Imamura, M., Hashimoto, T., Umeda, F., and Nawata, H. (2001) *Diabetologia* **44,** 614–620
20. Ragheb, R., Medhat, A. M., Shanab, G. M., Seoudi, D. M., and Fantus, I. G. (2008) *Biochem. Biophys. Res. Commun.* **370,** 134–139
21. Febbraio, M., and Silverstein, R. L. (2007) *Int. J. Biochem. Cell Biol.* **39,** 2012–2030
22. Belfrage, P., Jergil, B., Strälfors, P., and Tornqvist, H. (1978) *Adv. Exp. Med. Biol.* **101,** 113–126
23. Lingvay, I., Raskin, P., and Szczepaniak, L. S. (2009) *Nat. Rev. Cardiol.* **6,** 268–269
24. Hirano, K., Ikeda, Y., Zaima, N., Sakata, Y., and Matsumiya, G. (2008) *N. Engl. J. Med.* **359,** 2396–2398
25. Barnes, P. J., and Karin, M. (1997) *N. Engl. J. Med.* **336,** 1066–1071
26. Baeuerle, P. A., and Baltimore, D. (1988) *Science* **242,** 540–546
27. Finco, T. S., Beg, A. A., and Baldwin, A. S., Jr. (1994) *Proc. Natl. Acad. Sci. U.S.A.* **91,** 11884–11888
28. Müller, M., Morotti, A., and Ponzetto, C. (2002) *Mol. Cell. Biol.* **22,** 1060–1072
29. Schmitz, M. L., Bacher, S., and Dienz, O. (2003) *FASEB J.* **17,** 2187–2193
30. Kienesberger, P. C., Lee, D., Pulinilkunnil, T., Brenner, D. S., Cai, L., Magnes, C., Koefeler, H. C., Streith, I. E., Rechberger, G. N., Haemmerle, G., Flier, J. S., Zechner, R., Kim, Y. B., and Kershaw, E. E. (2009) *J. Biol. Chem.* **284,** 30218–30229
31. Wolf, B. A., Easom, R. A., Hughes, J. H., McDaniel, M. L., and Turk, J. (1989) *Biochemistry* **28,** 4291–4301
32. Kuroki, T., Inoguchi, T., Umeda, F., and Nawata, H. (1998) *Biochem. Biophys. Res. Commun.* **247,** 473–477
33. Baynes, J. W. (1991) *Diabetes* **40,** 405–412
34. Oberley, L. W. (1988) *Free Radic. Biol. Med.* **5,** 113–124
35. Ha, H., Kim, C., Son, Y., Chung, M. H., and Kim, K. H. (1994) *Free Radic. Biol. Med.* **16,** 271–274
36. Kakimoto, M., Inoguchi, T., Sonta, T., Yu, H. Y., Imamura, M., Etoh, T., Hashimoto, T., and Nawata, H. (2002) *Diabetes* **51,** 1588–1595
37. Wolff, S. P., Jiang, Z. Y., and Hunt, J. V. (1991) *Free Radic. Biol. Med.* **10,** 339–352
38. Inoguchi, T., Li, P., Umeda, F., Yu, H. Y., Kakimoto, M., Imamura, M., Aoki, T., Etoh, T., Hashimoto, T., Naruse, M., Sano, H., Utsumi, H., and Nawata, H. (2000) *Diabetes* **49,** 1939–1945
39. Tsubouchi, H., Inoguchi, T., Sonta, T., Sato, N., Sekiguchi, N., Kobayashi, K., Sumimoto, H., Utsumi, H., and Nawata, H. (2005) *Free Radic. Biol. Med.* **39,** 444–452

◆厚生労働省◆
難治性疾患克服研究事業 研究班
からのお願いです。

日本小児循環器学会
会員各位

2008年、わが国の心臓移植症例より、細胞内中性脂肪分解酵素欠損により心症状及びミオパチーを呈する新規疾患単位、中性脂肪蓄積心筋血管症（Triglyceride Deposit Cardiomyovasculopathy, TGCV)が、同定されました。現在のところ成人例しか同定されていませんが、発症から数年～10数年で、重症心不全を呈すると考えられるため、小児期での診断が重要と考えられます。

そこで会員の皆様に本疾患の概念・診断についてお知らせいたします。
もし、本疾患が疑わしい患者さんをご存じでしたら

東京慈恵会医科大学　井田博幸（email: hiroy@jikei.ac.jp),
或いは
大阪大学　平野賢一（email: khirano@cnt-osaka.com)

まで、ご連絡いただければ幸いです。宜しくお願い申し上げます。

平成24年3月

東京慈恵会医科大学　小児科　井田博幸
大阪大学医学部附属病院　循環器内科　平野賢一

“中性脂肪蓄積心筋血管症”
Triglyceride deposit cardiomyovasculopathy

(Hirano K, et al. N Engl J Med. 2008)

詳細は 裏面を
ご覧ください。

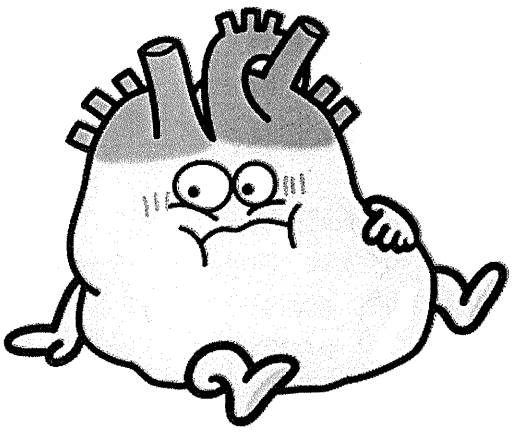

新しい疾患：
中性脂肪蓄積心筋血管症
Triglyceride Deposit Cardiomyovasculopathy (TGCV)
-知識の普及および早期発見に向けて-

＜疾患の紹介＞

2008年、我が国の心臓移植症例から見出された新規疾患であり（Hirano K, *et al.* N Engl J Med. 359: 2396-2398, 2008)、心筋、冠状動脈に中性脂肪が蓄積することにより心不全、不整脈、虚血性心疾患などを呈する。心筋症と診断されるケースが多い。20歳代から中年にかけて発症し数年から数十年で死にいたる難病。心外症状として骨格筋ミオパチーを呈するが症例によりその程度は異なる。現在のところ明らかな原因は、細胞内中性脂肪分解酵素 adipose triglyceride lipase (ATGL)の遺伝的欠損である。これまで、国内7症例（4例は20-50才代で心臓死、2例は、心臓移植）、国外16症例が見出されている。これまで報告された最若年例は、米国の18才女性で、心筋、骨格筋に中性脂肪蓄積を認めるものの心症状、骨格筋症状を認めない（Akman HO, *et al.* Neuromuscul Disord 20: 397-402, 2010)。

＜早期発見の必要性＞

上述のように20歳を過ぎると発症する可能性が出てくること、発症した時点でかなり進行している症例もいること、発症後、数年～10年数年で死に至ることより、10歳代のうちに発見されるべきである。

＜検査所見＞　成人では以下の所見が認められる。

1．末梢血塗抹標本にて、多核白血球、単球に著明な空胞変性（下図：Jordans' anomaly と呼ぶメイギムザ染色）が全症例で見られている。幼少時から見られるものであろうと推測される。

2．組織における中性脂肪の蓄積にも関わらず、血清中性脂肪値、カルニチンレベルなどは正常者と同様な値である。CPKが高値を示す症例はある。

3．研究班では、簡易スクリーニング法の開発バイオマーカーの探索に成功しております。ご興味のある先生方は、平野までご連絡をお願い申し上げます。

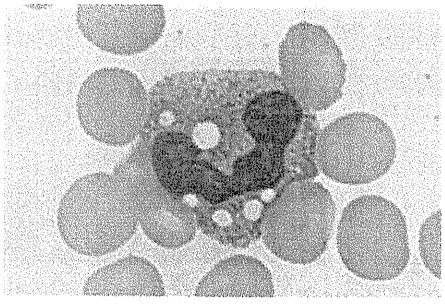

<治療＞

1．2症例に心臓移植が施行されている。

2．2症例に対して中鎖脂肪酸を含む食事療法が、大阪大学医学部附属病院において自主臨床研究として行われ、有効性が示唆されている。本療法の効果は、ATGL KOマウスにおいても確認された。酵素補充療法が理想的で、開発を促すため早期診断、症例数の把握が重要である。

ご協力のほど、何卒よろしくお願い申し上げます。

厚生労働省難治性疾患克服研究事業　中性脂肪蓄積心筋血管症　研究班
東京慈恵会医科大学　小児科　井田博幸　(小児領域研究代表者) (hiroy@jikei.ac.jp)
大阪大学医学部附属病院　循環器内科　　平野賢一　(総括研究代表者) (khirano@cnt-osaka.com)